Advances in Water Resources 32 (2009) 1601–1608

Contents lists available at ScienceDirect

Advances in Water Resources

journal homepage: www.elsevier.com/locate/advwatres

Two-dimensional stochastic analysis of flow in leaky confined aquifers subject to spatial and periodic leakage

Hund-Der Yeh *, Ching-Min Chang

Institute of Environmental Engineering, National Chiao Tung University, No. 75, Po-Ai Street, Hsinchu 300, Taiwan

ARTICLE INFO

Article history:
Received 12 February 2009
Received in revised form 16 August 2009
Accepted 17 August 2009
Available online 22 August 2009

Keywords:
Nonstationary spectral approach
Nonstationary head fields
Leaky confined aquifers
Heterogeneous media
Coefficient of leakage

ABSTRACT

This paper addresses the issue of flow in heterogeneous leaky confined aquifers subject to leakage. The leakage into the confined aquifer is driven by spatial and periodic fluctuations of water table in an overlying phreatic aquifer. The introduction of leakage leads to non-uniformity in the mean head gradient and results in nonstationarity in hydraulic head and velocity fields. Therefore, a nonstationary spectral approach based on Fourier–Stieltjes representations for the perturbed quantities is adopted to account for the spatial variability of nonstationary head fields. Closed-form expressions for the variances of hydraulic head and specific discharge are developed in terms of statistical properties of hydraulic parameters. The results indicate that the spatiotemporal variations in leakage leads to enhanced variability of the hydraulic head and of the specific discharge, which increase with distance from any arbitrary reference point. The coefficient of leakage and the spatial structure of log transmissivity field and of the amplitude of water table fluctuation are critical in quantifying the variability of the hydraulic head and of the specific discharge.

1. Introduction

Most of the existing stochastic analyses of groundwater flow in heterogeneous formations rely on the assumption of a constant mean head gradient in the treatment of flow problem. It is recognized that groundwater recharge may cause non-uniformity in the mean hydraulic head gradient, which results in nonstationarity in the statistics of random head fields in heterogeneous media [7,17]. Several studies [3,9,12,18] have revealed that the assumption of a uniform mean head gradient leads to the solution that fails to capture the covariances and cross-covariances in random nonstationary velocity fields. It is well known that the log conductivity-head cross-covariance is of significance in controlling the variability of flow-dependent variables such as hydraulic head. This implies that the applicability of solutions developed based on the uniform mean head gradient (or uniform mean flow) assumption to the quantification of the flow perturbation caused by the presence of recharge is excluded. Motivated by this, this study is devoted to the development of closed-form analytic expressions for quantifying the variability of hydraulic head and specific discharge in a leaky confined aquifer, where the stochastic nature of hydraulic head is unstationary.

The changes in groundwater table in response to a given temporal forcing are a common occurrence in many ground water basins. This temporal effect can directly affect the velocity variation and, therefore, the migration potential of contaminant plumes [6,10,16]. Therefore, to make correct groundwater management decisions, it is important to understand the temporal effect of recharge (leakage) on the mean behavior of flow system and the variability of the output processes (such as the variability of head and specific discharge). Several stochastic investigations of problems of flow and solute transport in a leaky confined aquifer have been presented over the past years [8,13,14,22,23]. However, to our knowledge, the application of the nonstationary spectral approach [11,12] to quantify the variability of hydraulic head and specific discharge in a leaky confined aquifer subject to spatial and periodic leakage has not been done so far. We hope that the approach in this study provides a basic framework for quantifying and understanding field-scale flow processes in heterogeneous leaky confined aquifers and the findings will be useful in stimulating further research in this area.

2. Mathematical formulation of the problem

Groundwater flow through a leaky confined aquifer overlain by a leaky phreatic aquifer is considered to be essentially horizontal, so that it can be modeled using the vertically integrated form of the continuity equation combined with Darcy's law [2]

* Corresponding author. Fax: +886 35 726050.
E-mail addresses: hdyeh@mail.nctu.edu.tw (H.-D. Yeh), changcm@mail.nctu.edu.tw (C.-M. Chang).

0309-1708/$ - see front matter © 2009 Elsevier Ltd. All rights reserved.
doi:10.1016/j.advwatres.2009.08.004

$$\frac{\partial}{\partial X_i}\left[T(\boldsymbol{X})\frac{\partial\phi(\boldsymbol{X},t)}{\partial X_i}\right]-\frac{\phi(\boldsymbol{X},t)-\phi_p(\boldsymbol{X},t)}{\zeta^2}=S\frac{\partial\phi(X,t)}{\partial t},\quad i=1,2 \tag{1}$$

where the leakage into the confined aquifer takes place through a leaky confining layer whose hydraulic conductivity is much smaller than that of the main aquifer. In Eq. (1), ϕ is the hydraulic head in the confined aquifer, ϕ_p is the hydraulic head in the phreatic aquifer, T is the transmissivity, S is the storativity and ζ^2 is the coefficient of leakage [2], which is defined as the root of the ratio of the thickness of the confining layer to its hydraulic conductivity. The conductivity of the confining layer does not vary significantly in space compared to the spatial variation of hydraulic conductivity in the confined aquifer. Therefore, the conductivity of the confining layer is assumed to be uniform. Expanding these terms in Eq. (1) and dividing the equation by the nonzero transmissivity yields

$$\frac{\partial^2\phi}{\partial X_i^2}+\frac{\partial\ln T}{\partial X_i}\frac{\partial\phi}{\partial X_i}-\frac{1}{T}\frac{\phi-\phi_p}{\zeta^2}=\frac{S}{T}\frac{\partial\phi}{\partial t} \tag{2}$$

The hydraulic head in the phreatic aquifer and log transmissivity $\ln T$ are regarded as realizations of stationary random fields perturbed into means and corresponding zero-mean perturbations

$$\begin{aligned}\phi_p(\boldsymbol{X},t)&=\langle\phi_p(\boldsymbol{X},t)\rangle+h_p(\boldsymbol{X},t)=H_p+h_p(\boldsymbol{X},t)\\ \ln T(\boldsymbol{X})&=\langle\ln T(\boldsymbol{X})\rangle+f(\boldsymbol{X})=F+f(\boldsymbol{X})\end{aligned} \tag{3}$$

where $\langle\rangle$ stands for the expected value operator. The random spatial fluctuations of $\ln T$ and the water table fluctuations in space and time result in random spatiotemporal variability of aquifer heads

$$\phi(\boldsymbol{X},t)=\langle\phi(\boldsymbol{X},t)\rangle+h(\boldsymbol{X},t)=H(\boldsymbol{X},t)+h(\boldsymbol{X},t) \tag{4}$$

where $h(\boldsymbol{X},t)$ is the zero-mean perturbation.

Substituting perturbation expansions (3) and (4) into Eq. (2), dropping all products of perturbations and subsequently taking the expected value in the resulting equation, one obtains a first-order approximation of the flow equation governing the mean hydraulic head

$$\frac{\partial^2H}{\partial X_i^2}-\frac{H-H_p}{e^F\zeta^2}=\frac{S}{e^F}\frac{\partial H}{\partial t} \tag{5}$$

where the variability of S is assumed negligible. Subtracting this mean equation from Eq. (2) leads to the following equation

$$\frac{\partial^2h}{\partial X_i^2}-\frac{h-h_p}{e^F\zeta^2}+\frac{\partial f}{\partial X_i}\frac{\partial H}{\partial X_i}+f\frac{H-H_p}{e^F\zeta^2}=\frac{S}{e^F}\frac{\partial h}{\partial t}-\frac{fS}{e^F}\frac{\partial H}{\partial t} \tag{6}$$

With reference to Eq. (5), a first-order partial differential equation relating the perturbations f and h is found as

$$\frac{\partial^2h}{\partial X_i^2}-\frac{h-h_p}{e^F\zeta^2}+\left[\frac{\partial f}{\partial X_i}\frac{\partial H}{\partial X_i}+f\frac{\partial^2H}{\partial X_i^2}\right]=\frac{S}{e^F}\frac{\partial h}{\partial t} \tag{7}$$

If the X_1 direction is selected to be in the direction of the mean flow, the equations for the mean head and perturbation can then be simplified to

$$\frac{\partial^2H}{\partial X_1^2}-\frac{H-H_p}{e^F\zeta^2}=\frac{S}{e^F}\frac{\partial H}{\partial t} \tag{8}$$

$$\frac{\partial^2h}{\partial X_i^2}-\frac{h-h_p}{e^F\zeta^2}+\left[\frac{\partial f}{\partial X_1}\frac{\partial H}{\partial X_1}+f\frac{\partial^2H}{\partial X_1^2}\right]=\frac{S}{e^F}\frac{\partial h}{\partial t} \tag{9}$$

Eqs. (8) and (9) provide the framework required to develop the first two moments of the hydraulic head and specific discharge in terms of the statistics of the input hydraulic parameters.

The perturbation expansion (first-order analysis) is an efficient and powerful method for solving the stochastic equation. This method is formally limited to relatively small variance ($\sigma_f^2\ll 1$, where σ_f^2 is the variance of $\ln T$). However, Zhang and Winter [21] found it to be accurate for the head variance solutions for σ_f^2 as high as 4.38. A similar finding was reported in Gelhar [4].

3. Spectral solutions

The approach followed is to solve Eq. (9) to fully characterize the second moments of hydraulic head and specific discharge. However, the mean Eq. (8) must be solved first in order to develop expressions for the products of mean hydraulic head gradients in Eq. (9).

3.1. Head variance

Suppose that the water table starts to fluctuate in response to periodic forcing (e.g., seasonal recharge or tides) and it would consist of a steady component (mean water table) plus a periodic perturbation. As such, the mean Eq. (8) for the flow would be time invariant and the solution to Eq. (8) can be shown to be

$$H(X_1)=H_p+(H_0-H_p)\cosh(\eta X_1)-\frac{J_0}{\eta}\sinh(\eta X_1) \tag{10}$$

where $\eta=1/(\zeta e^{F/2})$ and H_0 and J_0 are the reference mean head and negative mean head gradient at arbitrary location $X_1=0$, respectively. From Eq. (10), we immediately have

$$\frac{\partial H}{\partial X_1}=\eta(H_0-H_p)\sinh(\eta X_1)-J_0\cosh(\eta X_1) \tag{11}$$

$$\frac{\partial^2H}{\partial X_1^2}=\eta^2(H_0-H_p)\cosh(\eta X_1)-J_0\eta\sinh(\eta X_1) \tag{12}$$

Superposition is a useful tool in analyzing linear groundwater problems [19,20]. The principle of superposition states that a complex equation can be divided into sub-equations and the solution to the original equation is then obtained by summing the individual solution to each of the sub-equations. Based on this principle, the head perturbation in Eq. (9) can be separated conveniently into steady-state and time-varying components [19,20] such that

$$h(\boldsymbol{X},t)=h_s(\boldsymbol{X})+h_\tau(\boldsymbol{X},t) \tag{13}$$

This leads to separate differential equations for the steady and periodic components of head

$$\frac{\partial^2h_s}{\partial X_i^2}-\frac{h_s}{e^F\zeta^2}+\left[\frac{\partial f}{\partial X_1}\frac{\partial H}{\partial X_1}+f\frac{\partial^2H}{\partial X_1^2}\right]=0 \tag{14}$$

$$\frac{\partial^2h_\tau}{\partial X_i^2}-\frac{h_\tau-h_p}{e^F\zeta^2}=\frac{S}{e^F}\frac{\partial h_\tau}{\partial t} \tag{15}$$

The solutions to Eqs. (14) and (15) can be determined using Fourier–Stieltjes representations for the perturbed quantities [1,11,12]. By using this approach, the $\ln T$ perturbation field f is assumed to be a second-order stationary random field and represented by the following two-dimensional wave number integral:

$$f(\boldsymbol{X})=\int_{-\infty}^{\infty}e^{i\boldsymbol{K}\cdot\boldsymbol{X}}dZ_f(\boldsymbol{K}) \tag{16}$$

where $dZ_f(\boldsymbol{K})$ is the complex Fourier amplitude of $\ln T$ process, $\boldsymbol{K}=(K_1,K_2)$ is the wave number vector, and $K^2=K_1^2+K_2^2$.

The mean hydraulic head gradient is dependent of $\boldsymbol{X}$ as indicated in Eq. (11). This space-dependent mean head gradient causes the head random perturbations in Eq. (14) to be nonstationary. However, the head perturbed quantities in Eq. (14) can be presented using the nonstationary spectral representation [11,12] as

$$h_s(\boldsymbol{X})=\int_{-\infty}^{\infty}\Phi_{hf}(\boldsymbol{X},\boldsymbol{K})dZ_f(\boldsymbol{K}) \tag{17}$$

where $\Phi_{hf}(\boldsymbol{X},\boldsymbol{K})$ is a transfer function to be given. Thus substituting Eqs. (16) and (17) into Eq. (14) and invoking the uniqueness of the spectral representation gives the following equation

$$\frac{\partial^2\Phi_{hf}}{\partial X_i^2}-\eta^2\Phi_{hf}=\{\eta[-iK_1(H_0-H_p)+J_0]\sinh(\eta X_1)+[-\eta^2(H_0-H_p)+iJ_0K_1]\cosh(\eta X_1)\}e^{i\boldsymbol{K}\cdot\boldsymbol{X}} \tag{18}$$

The corresponding solution is

$$\Phi_{hf}(\boldsymbol{X},\boldsymbol{K})=J_0\left\{\eta R_1(\eta X_1)\frac{K^2-2K_1^2}{K^4+4\eta^2K_1^2}+iR_2(\eta X_1)\frac{(K^2+2\eta^2)K_1}{K^4+4\eta^2K_1^2}\right\}e^{i\boldsymbol{K}\cdot\boldsymbol{X}} \tag{19}$$

where $R_1(\eta X_1)=v\eta\cosh(\eta X_1)-\sinh(\eta X_1)$, $R_2(\eta X_1)=v\eta\sinh(\eta X_1)-\cosh(\eta X_1)$, $v=(H_0-H_p)/J_0$. Note that taking the advantage of a closed-form expression, the boundary effects on the perturbation h_s is assumed negligible [12,14] in obtaining the solution of (19). It is expected that the boundary effect is largely limited to a small zone next to the medium boundary.

Suppose that when $t>0$, the water table starts to fluctuate (as in response to a periodic forcing) according to

$$h_p(\boldsymbol{X},t)=h_{p_0}(\boldsymbol{X})\sin(\omega t) \tag{20}$$

where h_{p_0} is the amplitude of water-level fluctuation in the leaky phreatic aquifer and ω is the angular frequency. We consider h_{p_0} and h_τ as spatially correlated, stationary, random processes. Stationarity of the h_τ and h_{p_0} processes allows the Fourier–Stieltjes representations

$$h_\tau(\boldsymbol{X},t)=\int_{-\infty}^{\infty}e^{i\boldsymbol{K}\cdot\boldsymbol{X}}dZ_{h_\tau}(\boldsymbol{K},t) \tag{21}$$

$$h_{p_0}(\boldsymbol{X})=\int_{-\infty}^{\infty}e^{i\boldsymbol{K}\cdot\boldsymbol{X}}dZ_{h_p}(\boldsymbol{K}) \tag{22}$$

where dZ_{h_τ} and dZ_{h_p} are the complex Fourier amplitudes of h_τ and h_{p_0} processes, respectively.

The transient-state part of the spectral relation follows from Eq. (15) through the application of Eqs. (20)–(22) and the use of uniqueness of the representations:

$$\frac{d}{dt}dZ_{h_\tau}(\boldsymbol{K},t)+\frac{e^F}{S}(\eta^2+K^2)dZ_{h_\tau}(\boldsymbol{K},t)=\frac{e^F\eta^2}{S}\sin(\omega t)dZ_{h_p}(\boldsymbol{K}) \tag{23}$$

It is assumed that at $t=0$ the transient-state part of the head distribution is smooth, that is, $h_\tau(\boldsymbol{X},t=0)=0$. Thus, $dZ_{h_\tau}=0$ at $t=0$. The solution for (23) is then

$$dZ_{h_\tau}=\frac{e^F\eta^2}{S}\frac{-\omega\cos(\omega t)+\chi\sin(\omega t)+\omega e^{-\chi t}}{\chi^2+\omega^2}dZ_{h_p} \tag{24}$$

where $\chi=e^F(K^2+\eta^2)/S$. With Eq. (24), the time-varying component of head perturbation (21) is given by

$$h_\tau(\boldsymbol{X},t)=\eta^2\int_{-\infty}^{\infty}\frac{e^{i\boldsymbol{K}\cdot\boldsymbol{X}}}{(K^2+\eta^2)^2+\varpi^2}\left\{\sin(\omega t)\left[-\frac{\varpi}{\tan(\omega t)}+K^2+\eta^2\right]+\varpi e^{-\chi t}\right\}dZ_{h_p}(\boldsymbol{K}) \tag{25}$$

where $\varpi=\omega S/e^F$. The last term of the integrand in Eq. (25) which dies away as t becomes large.

Finally, the head perturbation in Eq. (13) is determined by integrals (17), (19) and (25) and the corresponding solutions for the steady and time-varying components of head variance can be expressed, respectively, as

$$\sigma_{h_s}^2(\boldsymbol{X})=J_0^2\left\{\eta^2R_1^2\int_{-\infty}^{\infty}\frac{(K^2-2K_1^2)^2}{(K^4+4\eta^2K_1^2)^2}S_{ff}(\boldsymbol{K})d\boldsymbol{K}+R_2^2\int_{-\infty}^{\infty}\frac{(K^2+2\eta^2)^2K_1^2}{(K^4+4\eta^2K_1^2)^2}S_{ff}(\boldsymbol{K})d\boldsymbol{K}\right\} \tag{26}$$

$$\sigma_{h_\tau}^2(t)=\eta^4\int_{-\infty}^{\infty}\left\{\sin(\omega t)\left[-\frac{\varpi}{\tan(\omega t)}+K^2+\eta^2\right]+\varpi e^{-\chi t}\right\}^2\times\frac{S_{h_ph_p}(\boldsymbol{K})}{[(K^2+\eta^2)^2+\varpi^2]^2}d\boldsymbol{K} \tag{27}$$

where $S_{ff}(\boldsymbol{K})$ is the spectrum of $\ln T$ and $S_{hphp}(\boldsymbol{K})$ is the spectrum of h_p. By noting that h_s and h_τ are statistically independent, the complete solution for the head variance is then given by

$$\sigma_h^2(\boldsymbol{X},t)=\sigma_{h_s}^2(\boldsymbol{X})+\sigma_{h_\tau}^2(t) \tag{28}$$

Eq. (28) is a local head variance relationship illustrating that the head variability is determined by the statistical properties of input hydraulic parameters.

3.2. Variance of specific discharge

The first-order equation for the specific discharge perturbation, which can be determined using Darcy's equation, takes the form [5]

$$q_i'=T_G\left[\delta_{i1}J(X_1)f-\frac{\partial h}{\partial X_i}\right] \tag{29}$$

where $T_G=\exp[F]$ and

$$J(X_1)=-\frac{\partial H}{\partial X_1}=J_0\cosh(\eta X_1)-\eta(H_0-H_p)\sinh(\eta X_1) \tag{30}$$

defined previously by Eq. (11). From Eqs. (13), (17), (19) and (25), the last term on the right-hand side of Eq. (29) in the X_1 direction can be written as

$$\frac{\partial h}{\partial X_1}=J_0\int_{-\infty}^{\infty}(\Omega_1+i\Omega_2)e^{i\boldsymbol{K}\cdot\boldsymbol{X}}dZ_f(\boldsymbol{K})+i\eta^2\int_{-\infty}^{\infty}\frac{e^{i\boldsymbol{K}\cdot\boldsymbol{X}}K_1}{[(K^2+\eta^2)^2+\varpi^2]^2}\times\left\{\sin(\omega t)\left[-\frac{\varpi}{\tan(\omega t)}+K^2+\eta^2\right]+\varpi e^{-\chi t}\right\}dZ_{h_p}(\boldsymbol{K}) \tag{31}$$

where

$$\Omega_1=R_2(\xi_1)\frac{-K^2K_1^2+\eta^2K^2-4\eta^2K_1^2}{K^4+4\eta^2K_1^2} \tag{32}$$

$$\Omega_2=2\eta R_1(\xi_1)\frac{K^2K_1-K_1^3+\eta^2K_1}{K^4+4\eta^2K_1^2} \tag{33}$$

Similarly, in the X_2 direction

$$\frac{\partial h}{\partial X_2}=\int_{-\infty}^{\infty}iK_2\Phi_{hf}(\boldsymbol{X},\boldsymbol{K})dZ_f(\boldsymbol{K})+i\eta^2\int_{-\infty}^{\infty}\frac{e^{i\boldsymbol{K}\cdot\boldsymbol{X}}K_2}{[(K^2+\eta^2)^2+\varpi^2]^2}\times\left\{\sin(\omega t)\left[-\frac{\varpi}{\tan(\omega t)}+K^2+\eta^2\right]+\varpi e^{-\chi t}\right\}dZ_{h_p}(\boldsymbol{K}) \tag{34}$$

where Φ_{hf} is defined previously by Eq. (19).

Substituting Eqs. (31) and (34) and the Fourier–Stieltjes representations of specific discharge perturbations, i.e.,

$$q_i'=\int_{-\infty}^{\infty}\exp[i\boldsymbol{K}\cdot\boldsymbol{X}]dZ_{q_i}(\boldsymbol{K}) \tag{35}$$

where $dZ_{q_i}(\boldsymbol{K})$ is the complex Fourier–Stieltjes amplitude of q_i', into the specific discharge perturbation Eq. (29) and invoking the uniqueness of the spectral representation gives the following specific discharge spectra in the longitudinal and transverse directions, respectively,

$$S_{q_1q_1}(\boldsymbol{K}) = S_{q_{1s}}(\boldsymbol{K}) + S_{q_{1\tau}}(\boldsymbol{K}) = T_G^2\left\{J_0^2[R_2^2(1+\Lambda_1)^2 + R_1^2\Lambda_2^2]S_{ff}(\boldsymbol{K}) + \left\{\sin(\omega t)\left[-\frac{\varpi}{\tan(\omega t)} + K^2 + \eta^2\right] + \varpi e^{-\chi t}\right\}^2 \times \frac{\eta^4 K_1^2 S_{h_ph_p}(\boldsymbol{K})}{[(K^2+\eta^2)^2+\varpi^2]^2}\right\} \tag{36}$$

$$S_{q_2q_2}(\boldsymbol{K}) = S_{q_{2s}}(\boldsymbol{K}) + S_{q_{2\tau}}(\boldsymbol{K}) = T_G^2\left\{J_0^2[R_2^2\Lambda_3^2 + R_1^2(\xi_1)\Lambda_4^2]S_{ff}(\boldsymbol{K}) + \left\{\sin(\omega t)\left[-\frac{\varpi}{\tan(\omega t)} + K^2 + \eta^2\right] + \varpi e^{-\chi t}\right\}^2 \times \frac{\eta^4 K_2^2 S_{h_ph_p}(K)}{[(K^2+\eta^2)^2+\varpi^2]^2}\right\} \tag{37}$$

where

$$\Lambda_1 = \frac{-K^2K_1^2 + \eta^2K^2 - 4\eta^2K_1^2}{K^4 + 4\eta^2K_1^2} \tag{38a}$$

$$\Lambda_2 = \frac{2\eta(K^2 - K_1^2 + \eta^2)K_1}{K^4 + 4\eta^2K_1^2} \tag{38b}$$

$$\Lambda_3 = \frac{K_1(K^2+2\eta^2)K_2}{K^4 + 4\eta^2K_1^2} \tag{39a}$$

$$\Lambda_4 = \frac{\eta(K^2 - 2K_1^2)K_2}{K^4 + 4\eta^2K_1^2} \tag{39b}$$

The expressions in Eqs. (36) and (37) contain two principal components depending on spatial fluctuations alone and both spatial and temporal fluctuations. Within the spectral framework, the specific discharge variance can be evaluated as

$$\sigma_{q_i}^2 = \sigma_{q_{iss}}^2 + \sigma_{q_{i\tau}}^2 = \int_{-\infty}^{\infty}[S_{q_{is}}(\boldsymbol{K}) + S_{q_{i\tau}}(\boldsymbol{K})]\boldsymbol{dK} \tag{40}$$

where the longitudinal and transverse components of integrand are defined by Eqs. (36) and (37), respectively.

4. Closed-form solutions

The variances of hydraulic head (28) and specific discharge (40) requires the knowledge of spectral density functions of f and h_p, we need to select them before using Eqs. (28) and (40). We consider the case where the random ln$T$ perturbation field can be represented by the following spectral density function [12,13,15]

$$S_{ff}(\boldsymbol{K}) = \frac{3\sigma_f^2\alpha^2K^4}{\pi(K^2+\alpha^2)^4} \tag{41}$$

where $\alpha = 3\pi/(16\lambda)$ and σ_f^2 and λ are the variance and integral scale of ln$T$, respectively. Note that the choice of (41) is to meet the mathematical requirement of zero spectral amplitude at zero wave number, and, therefore, in order to produce a finite-variance head process [4]. In addition, the spectral density function to characterize the amplitude of water table fluctuation in Eq. (20) is assumed to be described by Li and Graham [13]

$$S_{h_ph_p}(\boldsymbol{K}) = \frac{3\sigma_{h_p}^2\alpha_p^2K^4}{\pi(K^2+\alpha_p^2)^4} \tag{42}$$

where $\alpha_p = 3\pi/(16\lambda_p)$ and σ_{hp}^2 and λ_p are the variance and integral scale of the amplitude of water table fluctuation, respectively.

To simplify the analysis we assume that sufficient time has elapsed for the exponential term in Eq. (25) to die away (i.e., $e^{-\chi t} \to 0$). Because of $\varpi \ll 1$, corresponding to ranges of ω, S and e^F that are likely to be of interest, and the form of the denominator in Eq. (27), the approximate solution for the time-varying component of head variance (27) may be developed by neglecting the ϖ^2 term in the denominator. As a result

$$\sigma_{h_\tau}^2(t) = \eta^4\sin^2(\omega t)\int_{-\infty}^{\infty}\frac{\left[-\frac{\varpi}{\tan(\omega t)} + K^2 + \eta^2\right]^2}{(K^2+\eta^2)^4}S_{h_ph_p}(\boldsymbol{K})d\boldsymbol{K} \tag{43}$$

Similarly, the specific discharge spectra in the longitudinal and transverse directions (i.e., Eqs. (36) and (37)) can be approximated, respectively, as

$$S_{q_1q_1}(\boldsymbol{K}) = T_G^2\left\{J_0^2[R_2^2(1+\Lambda_1)^2 + R_1^2\Lambda_2^2]S_{ff}(\boldsymbol{K}) + \eta^4\sin^2(\omega t) \times \frac{K_1^2\left[\frac{-\varpi}{\tan(\omega t)} + K^2 + \eta^2\right]^2}{(K^2+\eta^2)^4}S_{h_ph_p}(\boldsymbol{K})\right\} \tag{44}$$

$$S_{q_2q_2}(\boldsymbol{K}) = T_G^2\left\{J_0^2\left[R_2^2\Lambda_3^2 + R_1^2(\xi_1)\Lambda_4^2\right]S_{ff}(\boldsymbol{K}) + \eta^4\sin^2(\omega t) \times \frac{K_2^2\left[\frac{-\varpi}{\tan(\omega t)} + K^2 + \eta^2\right]^2}{(K^2+\eta^2)^4}S_{h_ph_p}(\boldsymbol{K})\right\} \tag{45}$$

4.1. Head variance

Substituting Eqs. (41) and (42) into Eqs. (26) and (43) and integrating leads to the following expressions for the steady and time-varying components of head variance, depending on spatial fluctuations alone and both spatial and temporal fluctuations, respectively:

$$\sigma_{h_{sw}}^2 = \left(\frac{16}{3\pi}\right)^2J_0^2\lambda^2\sigma_f^2\left\{R_1^2(\beta\xi_1)\left[\frac{1}{(\Gamma^2-4)^4}\left(\frac{1}{2}\Gamma^6 + 13\Gamma^4 + 42\Gamma^2 + 12\right) - \frac{12}{(\Gamma^2-4)^{9/2}}\left(\Gamma^5 + 3\Gamma^3 + 8\Gamma - \frac{4}{\Gamma}\ln\left(\frac{1}{2}\Gamma + \sqrt{\Gamma^2/4-1}\right)\right)\right] + R_2^2(\beta\xi_1)\left[\frac{1}{(\Gamma^2-4)^4}\left(\frac{1}{4}\Gamma^8 - 5\Gamma^6 - 10\Gamma^4 - 4\Gamma^2 + 12\right) + \frac{6}{(\Gamma^2-4)^{9/2}}\left(5\Gamma^5 - 2\Gamma^3 - 4\Gamma + \frac{8}{\Gamma}\right)\ln\left(\frac{1}{2}\Gamma + \sqrt{\Gamma^2/4-1}\right)\right]\right\} \tag{46}$$

$$\sigma_{h_\tau}^2 = \sigma_{h_p}^2\sin^2(\omega t)\frac{\varepsilon^2}{(\varepsilon-1)^7}\{(\varepsilon-1)[1 + (8+20\mu+\mu^2)\varepsilon + (-18+18\mu+29\mu^2)\varepsilon^2 + (8-36\mu+29\mu^2)\varepsilon^3 + (-1+\mu)^2\varepsilon^4] - 6\varepsilon\ln[\varepsilon](\varepsilon-1)^2(1+\varepsilon) + (1+5\varepsilon-3\varepsilon^2-3\varepsilon^3)\mu + 2\varepsilon(1+3\varepsilon+\varepsilon^2)\mu^2]\} \tag{47}$$

where R_1 and R_2 are redefined, respectively, as $R_1(\beta\xi_1) = \nu\beta\cosh(\beta\xi_1)/\lambda - \sinh(\beta\xi_1)$, $R_2(\beta\xi_1) = \nu\beta\sinh(\beta\xi_1)/\lambda - \cosh(\beta\xi_1)$, $\beta = \lambda\eta, \xi_1 = X_1/\lambda, \Gamma = 3\pi/(16\beta)$, $\varepsilon = [(16/3\pi)\rho]^2, \rho = \lambda_p\eta, \eta = 1/(\zeta e^{F/2})$ and $\mu = S\omega\zeta^2/\tan(\omega t)$.

The behavior of the dimensionless steady component of head variance in Eq. (46) as a function of dimensionless position for various β is presented graphically in Fig. 1a. It indicates that the head variance increases with position, while it decreases with the coefficient of leakage ζ^2, which is inversely related to $\beta(=\lambda/(\zeta e^{F/2}))$, for fixed values of e^F and λ at a fixed location. Note that a larger coefficient of leakage leads to less leakage into the confined aquifer. The increase in the head variance with decreasing ζ at a fixed location can be explained by the fact that a decrease in ζ produces

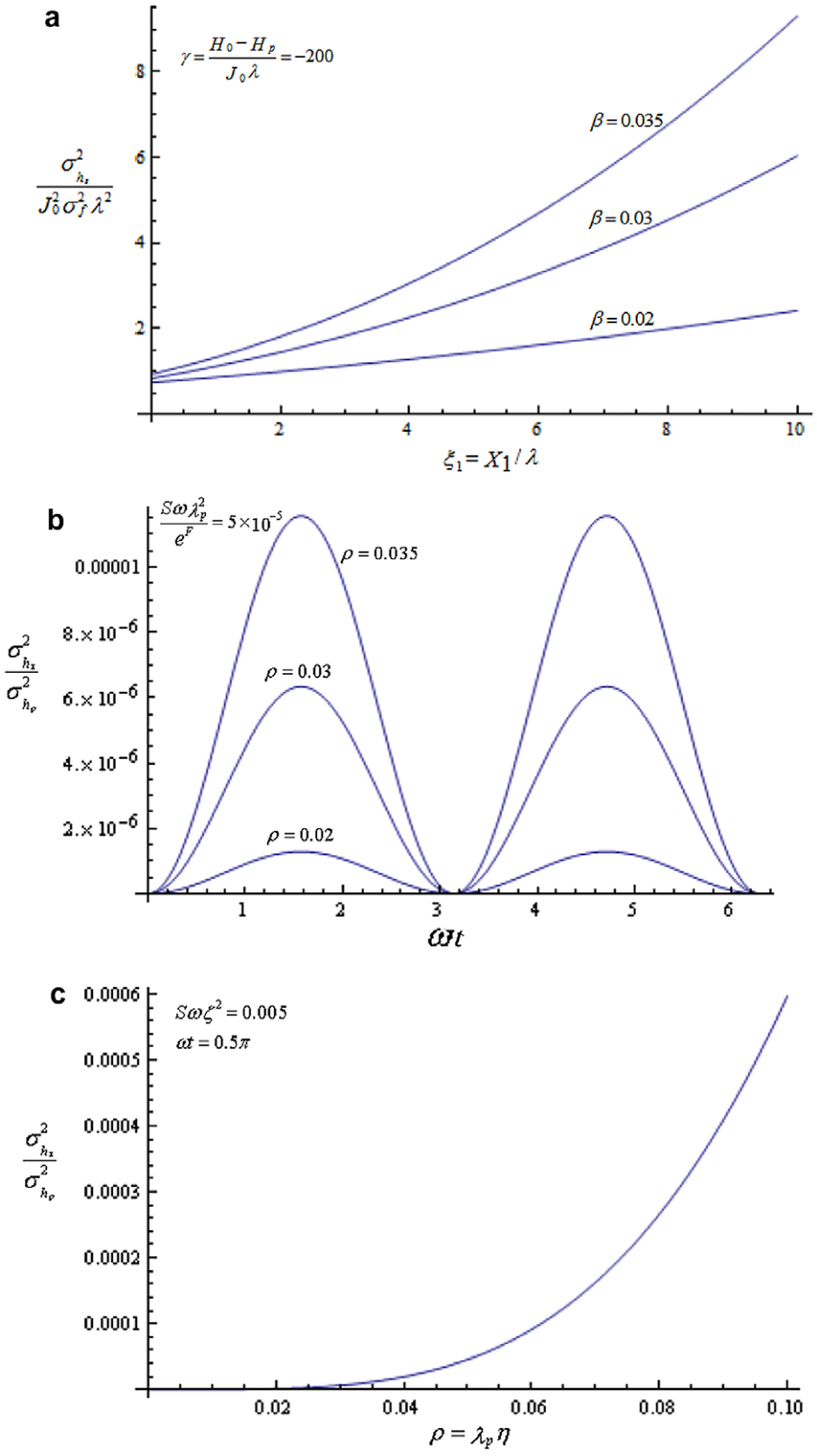

Fig. 1. (a) Dimensionless steady component of head variance as a function of dimensionless position. Dimensionless time-varying component of head variance as a function of (b) dimensionless time and (c) dimensionless integral scale of the amplitude of water table fluctuation.

more persistence of head fluctuations, which leads to larger deviations of the head from the mean head surface. Fig. 1b depicts the behavior of the dimensionless time-varying component of head variance in Eq. (47) as a function of dimensionless time. It can be clearly seen the reduction in hydraulic head variability with increasing ζ for fixed values of e^F and λ_p at a specified time. As expected, the increase in the time-varying component of head variance with λ_p is shown in Fig. 1c. The increase in the scaled time-varying component of head variance is generally with ρ, due to either decreasing coefficient of leakage, because of greater

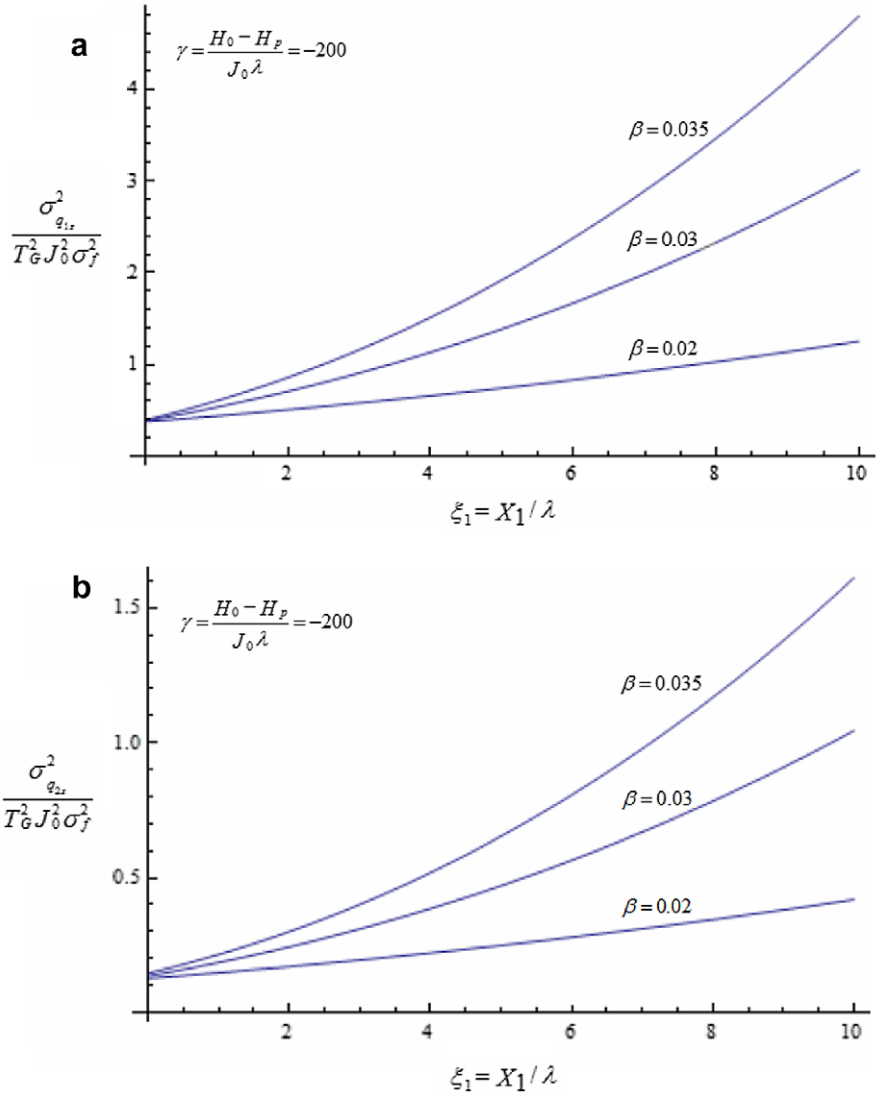

Fig. 2. Dimensionless steady components of specific discharge variance (a) in the longitudinal direction and (b) in the transverse direction as a function of dimensionless position. Dimensionless time-varying component of specific discharge variance in the longitudinal direction as a function of (c) dimensionless time and (d) dimensionless integral scale of the amplitude of water table fluctuation.

communication with the overlying water table, or due to increasingly spatially correlated water table fluctuations. The latter implies that water table fluctuations are either consistently above or below zero, thus contributing to a greater head variance. Finally, we note that in the limit of $\beta \to 0$ (i.e., $\zeta \to \infty$), corresponding to the case of no leakage, Eq. (46) converges to $[8/(3\pi)]^2 J_0^2\sigma_f^2\lambda^2$, which is identical to Eq. (21) of Mizell et al. [15]. On the other hand, for the no leakage case ($\zeta \to \infty$) the two aquifer are hydraulically disconnected, therefore, the time-varying component of head variance in Eq. (47) reduces to zero.

4.2. Variance of specific discharge

With Eqs. (41) and (42), closed-form solutions for the steady and time-varying components of specific discharge variance in the longitudinal and transverse directions are obtained by substituting Eqs. (36) and (37) into Eq. (40), respectively, and integrating them over the wave number domain

$$\sigma^2_{q_{1s}} = T_G^2J_0^2\sigma_f^2\left\{R_2^2(\beta\xi_1)(1+\Phi_1+\Phi_2)+R_1^2(\beta\xi_1)\Phi_3\right\} \tag{48}$$

$$\sigma^2_{q_{2s}} = T_G^2J_0^2\sigma_f^2\left\{R_2^2(\beta\xi_1)\Phi_4+R_1^2(\beta\xi_1)\Phi_5\right\} \tag{49}$$

$$\begin{aligned}\sigma^2_{q_{1\tau}} = \sigma^2_{q_{2\tau}} &= T_G^2\sigma^2_{h_p}\sin^2(\omega t)\frac{\eta^2\varepsilon}{4(\varepsilon-1)^7}\\ &\times\{-(\varepsilon-1)[-1+2(5+2\mu)\varepsilon+2\mu(36+11\mu)\varepsilon^2\\ &+(-26-36\mu+76\mu^2)\varepsilon^3+(17-40\mu+22\mu^2)\varepsilon^4]\\ &+6\varepsilon^2\ln[\varepsilon](\varepsilon-1)^2(3+\varepsilon)-2\mu(-3-3\varepsilon+5\varepsilon^2+\varepsilon^3)\\ &+(1+9\varepsilon+9\varepsilon^2+\varepsilon^3)\mu^2]\}\end{aligned} \tag{50}$$

where

$$\begin{aligned}\Phi_1 &= -2+\frac{11}{4}\Gamma^2+3\Gamma^2\ln[\Gamma]+\frac{1}{(\Gamma^2-4)^3}\\ &\times\left(-\frac{11}{4}\Gamma^8+29\Gamma^6-86\Gamma^4-16\Gamma^2-12\right)\\ &+\frac{1}{(\Gamma^2-4)^{7/2}}\left\{\left(-\frac{3}{2}\Gamma^9+21\Gamma^7-105\Gamma^5+210\Gamma^3\right)\right.\\ &\times\left(\ln\left[1+2\sqrt{\Gamma^2/4-1}/\Gamma\right]-\ln\left[1-2\sqrt{\Gamma^2/4-1}/\Gamma\right]\right)\\ &\left.-\left(168\Gamma+\frac{48}{\Gamma}\right)\ln\left[\frac{\Gamma}{2}+\sqrt{\Gamma^2/4-1}\right]\right\}\\ &+\frac{2}{(\Gamma^2-4)^4}(\Gamma^8-17\Gamma^6+118\Gamma^4-264\Gamma^2)\end{aligned} \tag{51a}$$

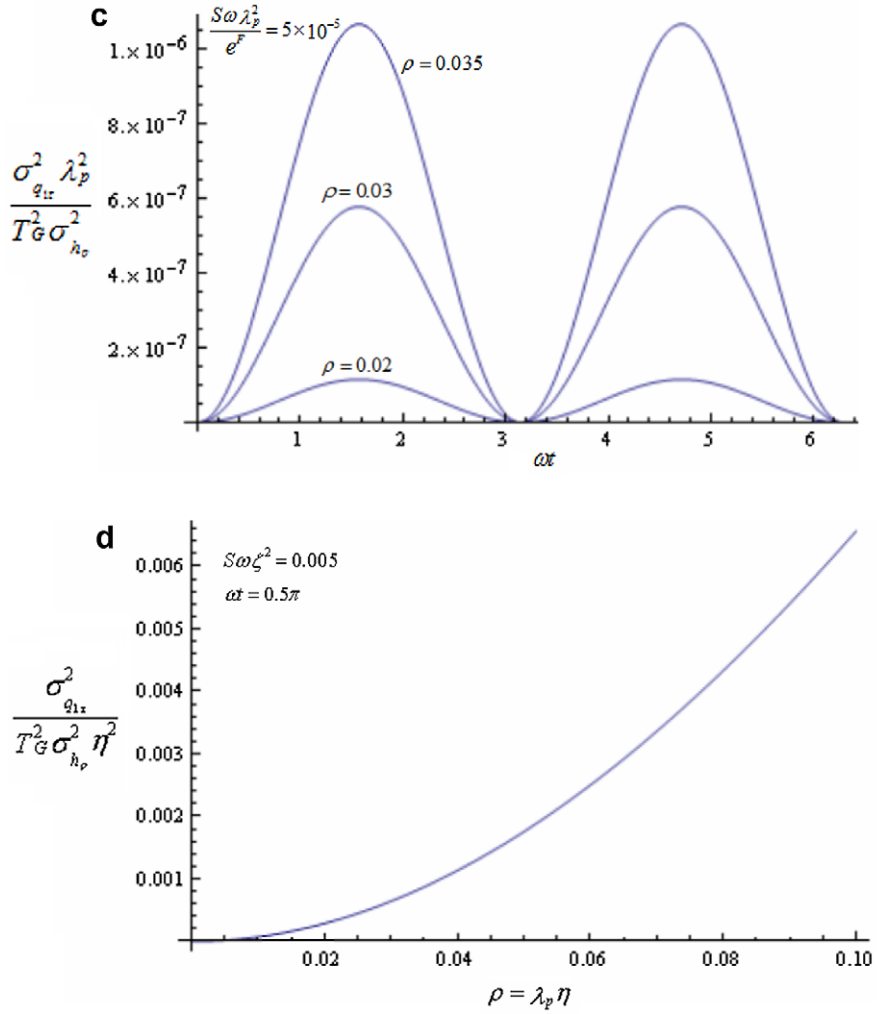

Fig. 2 (*continued*)

$$\Phi_2=-\frac{11}{4}\Gamma^2+\frac{13}{16}\Gamma^4+3\Gamma^2(\Gamma^2/2-1)\ln[\Gamma]+\frac{1}{(\Gamma^2-4)^4}\times\left(-\frac{13}{16}\Gamma^{12}+\frac{57}{4}\Gamma^{10}-\frac{775}{8}\Gamma^8+\frac{1237}{4}\Gamma^6-409\Gamma^4+42\Gamma^2+222+\frac{12}{\Gamma^2}\right)+\frac{1}{(\Gamma^2-4)^{9/2}}\left\{\left(-\frac{3}{4}\Gamma^{13}+15\Gamma^{11}-\frac{243}{2}\Gamma^9+504\Gamma^7-\frac{2205}{2}\Gamma^5+1260\Gamma^3\right)\times\left(\ln\left[1+2\sqrt{\Gamma^2/4-1}/\Gamma\right]-\ln\left[1-2\sqrt{\Gamma^2/4-1}/\Gamma\right]\right)-\left(300\Gamma^3+552\Gamma+\frac{144}{\Gamma}-\frac{48}{\Gamma^3}\right)\ln\left[\frac{\Gamma}{2}+\sqrt{\Gamma^2/4-1}\right]\right\} \tag{51b}$$

$$\Phi_3=\Gamma^2\left(-\frac{13}{8}\Gamma^2+\frac{33}{16}+\left(\frac{9}{4}-3\Gamma^2\right)\ln[\Gamma]\right)+\frac{1}{(\Gamma^2-4)^4}\left(\frac{13}{8}\Gamma^{12}-\frac{401}{16}\Gamma^{10}+\frac{573}{4}\Gamma^8-\frac{1421}{4}\Gamma^6+303\Gamma^4+59\Gamma^2-120+\frac{12}{\Gamma^2}\right)+\frac{1}{(\Gamma^2-4)^{9/2}}\times\left\{\left(\frac{3}{2}\Gamma^{13}-\frac{225}{8}\Gamma^{11}+\frac{837}{4}\Gamma^9-\frac{3087}{4}\Gamma^7+\frac{2835}{2}\Gamma^5-1260\Gamma^3\right)\times\left(\ln\left[1+2\sqrt{\Gamma^2/4-1}/\Gamma\right]-\ln\left[1-2\sqrt{\Gamma^2/4-1}/\Gamma\right]\right)+\left(348\Gamma^3+384\Gamma+\frac{24}{\Gamma}+\frac{48}{\Gamma^3}\right)\ln\left[\frac{\Gamma}{2}+\sqrt{\Gamma^2/4-1}\right]\right\} \tag{51c}$$

$$\Phi_4=\frac{11}{8}\Gamma^2-\frac{13}{16}\Gamma^4+\frac{3}{2}\Gamma^2(1-\Gamma^2)\ln[\Gamma]+\frac{1}{(\Gamma^2-4)^4}\times\left(\frac{13}{16}\Gamma^{12}-\frac{103}{8}\Gamma^{10}+\frac{615}{8}\Gamma^8-\frac{829}{4}\Gamma^6+\frac{449}{2}\Gamma^4-25\Gamma^2-52\right)+\frac{1}{(\Gamma^2-4)^{9/2}}\left\{\left(\frac{3}{4}\Gamma^{13}-\frac{57}{4}\Gamma^{11}+108\Gamma^9-\frac{819}{2}\Gamma^7+\frac{1575}{2}\Gamma^5-630\Gamma^3\right)\left(\ln\left[1+2\sqrt{\Gamma^2/4-1}/\Gamma\right]-\ln\left[1-2\sqrt{\Gamma^2/4-1}/\Gamma\right]\right)+\left(-72\Gamma^3+276\Gamma+\frac{48}{\Gamma}\right)\times\ln\left[\frac{\Gamma}{2}+\sqrt{\Gamma^2/4-1}\right]\right\} \tag{52a}$$

$$\Phi_5=-\frac{33}{16}\Gamma^2+\frac{13}{8}\Gamma^4+3\Gamma^2\left(\Gamma^2-\frac{3}{4}\right)\ln[\Gamma]+\frac{1}{(\Gamma^2-4)^4}\times\left(-\frac{13}{8}\Gamma^{12}+\frac{401}{16}\Gamma^{10}-\frac{573}{4}\Gamma^8+\frac{711}{2}\Gamma^6-307\Gamma^4-47\Gamma^2+12\right)+\frac{1}{(\Gamma^2-4)^{9/2}}\left\{\left(-\frac{3}{2}\Gamma^{13}+\frac{225}{8}\Gamma^{11}-\frac{837}{4}\Gamma^9+\frac{3087}{4}\Gamma^7-\frac{2835}{2}\Gamma^5+1260\Gamma^3\right)\left(\ln\left[1+2\sqrt{\Gamma^2/4-1}/\Gamma\right]-\ln\left[1-2\sqrt{\Gamma^2/4-1}/\Gamma\right]\right)-\left(342\Gamma^3+324\Gamma-\frac{48}{\Gamma}\right)\times\ln\left[\frac{\Gamma}{2}+\sqrt{\Gamma^2/4-1}\right]\right\} \tag{52b}$$

Fig. 2a and b shows how the dimensionless steady components of specific discharge variance in the longitudinal and transverse directions, respectively, vary with dimensionless position for various β. These figures suggest that decreasing the coefficient of leakage or increasing geometric mean of aquifer transmissivity increase the variability of specific discharge in the longitudinal and transverse directions at a fixed location. The increase in the dimensionless time-varying component of specific discharge variance in the longitudinal direction with ρ is displayed in Fig. 2c. Fig. 2d depicts the dependence of time-varying component of specific discharge variance in the longitudinal direction on the integral scale of the amplitude of water table fluctuation and indicates that the variability of time-varying component of specific discharge increases with the integral scale of the amplitude of water table fluctuation or with decreasing coefficient of leakage.

It is clear that in the case of no leakage ($\beta \to 0$), the steady components of specific discharge variance, Eqs. (48) and (49), respectively, reduce to

$$\sigma^2_{q_{1s}} = \frac{3}{8} T_G^2 J_0^2 \sigma_f^2 \tag{53}$$

$$\sigma^2_{q_{2s}} = \frac{1}{8} T_G^2 J_0^2 \sigma_f^2 \tag{54}$$

which are well-known expressions for two-dimensional flow reported in the literature. In addition, the time-varying component of specific discharge variance reduces to zero as $\zeta \to \infty$.

5. Conclusions

We have analyzed groundwater flow in heterogeneous leaky confined aquifers subject to leakage from a stochastic point of view. The leakage is driven by spatial and periodic fluctuations of the water table in an overlying phreatic aquifer. The presence of leakage affects the mean hydraulic head gradient and thereby causes nonstationarity in the statistics of hydraulic head fields. Closed-form expressions for the variances of hydraulic head and specific discharge are developed in terms of statistical properties of hydraulic parameters based on the perturbation approximation and spectral Fourier–Stieltjes nonstationary representations for the perturbed quantities.

The analyses in this study are limited to small perturbations in hydraulic properties, assuming that σ_f^2 is smaller than unit so that second-order terms in the flow equation can be neglected. For a larger σ_f^2, the adequacy of the first-order approximation is uncertain.

The results indicate that the introduction of spatial and temporal variations in leakage leads to enhanced and periodic variability of the hydraulic head and of the specific discharge, which increase with distance from any arbitrary reference point. The larger the coefficient of leakage, the less variability of the hydraulic head and of specific discharge. The variability of the time-varying component of hydraulic head and of specific discharge increases with the integral scale of the amplitude of water table fluctuation.

Acknowledgements

Research leading to this work has been supported by "Aim for the Top University Plan" of the National Chiao Tung University and Ministry of Education, Taiwan. We are grateful to the five anonymous reviewers for constructive comments that improved the quality of the work.

References

[1] Bakr AA, Gelhar LW, Gutjahr AL, MacMillan JR. Stochastic analysis of spatial variability in subsurface flows: 1. Comparison of one- and three-dimensional flows. Water Resour Res 1978;14(2):263–71.
[2] Bear J. Hydraulics of groundwater. New York, NY: McGraw-Hill; 1979.
[3] Chang C-M, Yeh H-D. Large-time behavior of macrodispersion in heterogeneous trending aquifers. Water Resour Res 2007;43:W11501. doi:10.1029/2007WR006017.
[4] Gelhar LW. Stochastic subsurface hydrology. Englewood Cliffs, New Jersey: Prentice Hall; 1993.
[5] Gelhar LW, Axness CL. Three-dimensional stochastic analysis of macrodispersion in aquifers. Water Resour Res 1983;19(1):161–80.
[6] Dagan G, Bellin A, Rubin Y. Lagrangian analysis of transport in heterogeneous formations under transient conditions. Water Resour Res 1996;32(4):891–9.
[7] Destouni G, Graham W. Solute transport through an integrated heterogeneous soil–groundwater system. Water Resour Res 1995;31(8):1935–44.
[8] Hantush MM, Marino MA. One-dimensional stochastic analysis in leaky aquifers subject to random leakage. Water Resour Res 1994;30(2):549–58.
[9] Indelman P, Rubin Y. Flow in heterogeneous media displaying a linear trend in the log conductivity. Water Resour Res 1995;31(5):1257–65.
[10] Kim K, Anderson MP, Bowser CJ. Enhanced dispersion in groundwater caused by temporal changes in recharge rate and lake levels. Adv Water Resour 2000;23(6):625–35.
[11] Li S-G, McLaughlin D. A nonstationary spectral method for solving stochastic groundwater problems: unconditional analysis. Water Resour Res 1991;27(7):1589–605.
[12] Li S-G, McLaughlin D. Using the nonstationary spectral method to analyze flow through heterogeneous trending media. Water Resour Res 1995;31(3):541–51.
[13] Li L, Graham WD. Stochastic analysis of solute transport in heterogeneous aquifers subject to spatiotemporal random recharge. Water Resour Res 1999;35(4):953–71.
[14] Lu G, Zhang D. Nonstationary stochastic analysis of flow in a heterogeneous semiconfined aquifer. Water Resour Res 2002;38(8):1155. doi:10.1029/2001WR000546.
[15] Mizell SA, Gutjahr AL, Gelhar LW. Stochastic analysis of spatial variability in two-dimensional steady groundwater flow assuming stationary and nonstationary heads. Water Resour Res 1982;18(4):1053–67.
[16] Rehfeldt KR, Gelhar LW. Stochastic analysis of dispersion in unsteady flow in heterogeneous aquifers. Water Resour Res 1992;28(8):2085–99.
[17] Rubin Y, Bellin A. The effects of recharge on flow nonuniformity and macrodispersion. Water Resour Res 1994;30(4):939–48.
[18] Rubin Y, Seong K. Investigation of flow and transport in certain cases of nonstationary conductivity fields. Water Resour Res 1994;30(11):2901–11.
[19] Townley LR. The response of aquifers to periodic forcing. Adv Water Resour 1995;18(3):125–46.
[20] Trefry MG. Periodic forcing in composite aquifers. Adv Water Resour 1999;22(6):645–56.
[21] Zhang D, Winter CL. Moment equation approach to single phase fluid flow in heterogeneous reservoirs. Soc Petrol Eng J 1999;4(2):118–27.
[22] Zhu J. Specific discharge covariance in a heterogeneous semiconfined aquifer. Water Resour Res 1998;34(8):1951–7.
[23] Zhu J, Sykes JF. Head variance and macrodispersivity tensor in a semiconfined fractal porous medium. Water Resour Res 2000;36(1):203–12.